



Published in final edited form as:

*J Am Chem Soc.* 2012 December 19; 134(50): 20211–20213. doi:10.1021/ja309863n.

## Improved Precursor Chemistry for the Synthesis of III-V Quantum Dots

Daniel K. Harris<sup>a</sup> and Mounji G. Bawendi<sup>b,\*</sup>

<sup>a</sup>Department of Materials Science and Engineering, Massachusetts Institute of Technology, 77 Massachusetts Avenue, Cambridge, MA 02139

<sup>b</sup>Department of Chemistry, Massachusetts Institute of Technology, 77 Massachusetts Avenue, Cambridge, MA 02139

### Abstract

The synthesis of III-V Quantum Dots has been long known to be more challenging than the synthesis of other types of inorganic quantum dots. This is attributed to highly reactive group-V precursors. We synthesized molecules that are suitable for use as group-V precursors and characterized their reactivity using multiple complementary techniques. We show that the size distribution of indium arsenide quantum dots indeed improves with decreased precursor reactivity.

Indium phosphide (InP) and indium arsenide (InAs) quantum dots (QDs) have proven difficult to synthesize with the narrow size distributions characteristic of cadmium selenide (CdSe) and lead selenide (PbSe) QDs.<sup>1</sup> InP QDs are of interest for applications that require cadmium-free, visible-emitting quantum dots, while InAs is of interest for applications involving near infrared emission. Rapid precursor conversion rates for the group-V precursors used in InP and InAs QD synthesis are believed to prevent the formation of highly monodisperse QD ensembles.<sup>1</sup> In this work, we identify less reactive precursors for phosphorous and arsenic containing QDs and show that they can enable the synthesis of QDs with narrower size distributions than existing precursors.

Walker and Allen's study<sup>1</sup> of the InP QD growth mechanism revealed that the role of precursor conversion in the growth of InP QDs is fundamentally different than the role of precursor conversion in the growth of CdSe<sup>2</sup> and PbSe<sup>3</sup> QDs. In particular, it was found that the selenium precursor conversion rate limits the formation and growth of CdSe and PbSe QDs, while the phosphorous precursor conversion precedes InP particle growth. Following precursor conversion, InP QD growth proceeds via a ripening process associated with a broadening of the particle size distribution.<sup>1–6</sup>

Despite the perceived importance of precursor reactivity for the synthesis of high quality QDs, little progress has been made toward the development of less reactive group-V precursors. To date, most reports of high quality III-V QDs have used tris(trimethylsilyl)arsine (TMSi<sub>3</sub>As) or tris(trimethylsilyl)phosphine (TMSi<sub>3</sub>P) as a group-V source. Joung et al. reported that by using tris(*tert*-butyldimethylsilyl) phosphine, they were

Corresponding Author: mgb@mit.edu.

The authors declare no competing financial interests.

#### Supporting Information

Detailed synthetic information; characterization of QDs by UV-Vis Absorbance spectroscopy, PL, TEM, and XRD; and characterization of precursors by NMR and FTIR is available in the supporting information. This material is available free of charge via the Internet at <http://pubs.acs.org>.

able to make larger InP QDs than by using  $\text{TMSi}_3\text{P}$ .<sup>7</sup> However, they did not attempt to characterize the precursor reactivity, nor did they show an improvement in size distribution.

We wanted to see if we could reduce precursor reactivity by using a group-V source that did not contain a labile Si-P or Si-As bond. A previous study of tris(trimethyl-group-IV) stibines mentioned that the thermal and air stability of the stibines increased as the group-IV element changed from silicon to germanium to tin.<sup>8</sup> We speculated that tris(trimethylgermyl)arsine and tris(trimethylstannyl)arsine and their phosphorous analogues might be less reactive precursors for the synthesis of III-V QDs. We have synthesized these molecules and used them to make InAs and InP quantum dots. We have also measured their reaction kinetics using UV-Vis and NMR spectroscopy.

Tris(trimethylsilyl)arsine ( $\text{TMSi}_3\text{As}$ ) and the similar molecules  $\text{TME}_3\text{V}$  (E=Si, Ge; V=P, As) were synthesized for evaluation as QD precursors. Previous syntheses of  $\text{TMGe}_3\text{V}$  have relied on the direct reaction of chlorotrimethylgermane ( $\text{TMGeCl}$ ) with  $(\text{NaK})_3(\text{P, As})$ .<sup>8</sup> Instead, we synthesized  $\text{TME}_3\text{V}$  from  $\text{TMSi}_3\text{V}$  using an adaptation of a technique previously used to synthesize  $\text{TMGe}_3\text{Sb}$  and  $\text{TMSn}_3\text{Sb}$  from  $\text{TMSi}_3\text{Sb}$ .<sup>9</sup>  $\text{TMGe}_3\text{As}$  was synthesized by mixing  $\text{TMSi}_3\text{As}$  with an excess of  $\text{TMGeCl}$  and heated. Because the boiling point of chlorotrimethylsilane ( $\text{TMSiCl}$ ) is lower than that of  $\text{TMGeCl}$  the exchange is driven to completion as the  $\text{TMSiCl}$  is distilled off of the reaction mixture to leave the desired product. This procedure was also adapted to make  $\text{TMSn}_3\text{As}$  and  $\text{TMSn}_3\text{P}$ . Details are available in the supporting information.

In order to determine if these molecules would be useful for synthesizing high quality colloidal quantum dots, QDs were prepared by reaction with indium(III) myristate ( $\text{InMy}_3$ ) using the different group-V sources under otherwise identical conditions (see supporting information for details).<sup>10</sup> Aliquots were removed from the growth solution and characterized by measuring absorbance spectra (figure 1a–d). In order to ensure that the results were as comparable as possible, all experimental parameters were kept the same (stirring rate, flask size, etc). Additional details are given in the supporting information. The absorption spectra for the aliquots from the indium phosphide solutions prepared using  $\text{TMGe}_3\text{P}$  and  $\text{TMSi}_3\text{P}$  were similar (the absorption peak from the  $\text{TMGe}_3\text{P}$  sample was slightly better defined), however the absorption spectra from the aliquots from the indium arsenide solutions prepared from  $\text{TMGe}_3\text{As}$  showed significantly better defined features than those prepared from  $\text{TMSi}_3\text{As}$  (the HWHM of QDs prepared from  $\text{TMGe}_3\text{As}$  is 37nm (101meV) vs. 45nm (120meV) for  $\text{TMSi}_3\text{As}$ , a 21% difference). The sharp features in the absorption spectrum are an indication of a narrow particle size distribution, suggesting that the indium arsenide particles prepared from  $\text{TMGe}_3\text{As}$  are more monodisperse than those prepared from the  $\text{TMSi}_3\text{As}$ . Particles synthesized in this way were further characterized by photoluminescence, transmission electron microscopy (TEM), and X-ray diffraction (XRD) (figures S1-S4). Attempting the same synthesis using  $\text{TMSn}_3\text{P}$  and  $\text{TMSn}_3\text{As}$  did not produce QD samples with sharp absorption features.

During QD synthesis, it was observed that the color change that occurred upon injection of group-V precursor seemed to occur smoothly over several seconds for the  $\text{TMGe}_3\text{V}$  precursors, while nearly instantaneously for the  $\text{TMSi}_3\text{V}$  precursors. In order to quantify this observation, an absorption dip probe was used to measure the rise in absorbance after precursor injection at 130°C, the injection temperature used for QD growth in figure 1. Previous experiments have indicated that the extinction coefficient of quantum dots in the UV region scales with particle volume.<sup>4,11</sup> Thus we used the absorbance at 310nm to monitor the formation of InAs and InP clusters (figure 2a–b). Although the absorbance in the UV rose quickly, the particles did not show absorption features without heating at elevated temperature (figure S5). In order to directly compare the rate of absorbance rise

upon injection of the two different precursors, a large excess of indium(III) myristate was used and the  $\text{TMGe}_3\text{As}$  and  $\text{TMSi}_3\text{As}$  solutions were injected alternately. This eliminated any source of error from variations in concentration. The absorbance rise appeared to be insensitive to when in the injection sequence they occurred. When the absorbance traces were normalized by the intensity change and overlaid for comparison, the two traces for each precursor were nearly identical (figure 2b–c). These results clearly show that the particle formation occurs more slowly for the  $\text{TMGe}_3\text{V}$  precursors than for the  $\text{TMSi}_3\text{V}$  precursors, suggesting that the precursor conversion is the rate limiting step in small particle or cluster formation—at least for particles synthesized using the  $\text{TMGe}_3\text{V}$  precursors. In fact, the absorbance rise for the  $\text{TMSi}_3\text{V}$  based precursor occurs on a timescale that is competitive with the time required for mixing (figure S6). Although these data clearly show that the absorbance rise is much slower for the  $\text{TMGe}_3\text{V}$  precursors than for the  $\text{TMSi}_3\text{V}$  precursors, the data are difficult to directly attribute to molecular precursor conversion. In order to compare the rates of molecular precursor conversion, NMR spectroscopy was used to monitor the evolution of precursor concentration in time.

An NMR tube was loaded with  $\text{InMy}_3$  and tri-n-octylphosphine (TOP). Just before the NMR tube was inserted into the instrument, a solution containing both group-V precursors was injected. A time series of NMR spectra (figure 3a) shows that the  $\text{TMSi}_3\text{P}$  peak disappears much faster than the  $\text{TMGe}_3\text{P}$  peak. The reaction was performed under pseudo-first order conditions, where the concentration of indium was  $>10\text{X}$  that of the phosphorous and arsenic. Exponential fits to the data indicate that under these conditions the reaction rate of  $\text{TMSi}_3\text{P}$  is more than 4x faster than the reaction rate of  $\text{TMGe}_3\text{P}$ . The concentration of  $\text{TME}_3\text{P}$  over time was consistent with a reaction with first order dependence on phosphorous precursor (figure 3b). An intermediate was observed (figure 3a) that is believed to be similar to that reported for the reaction of  $\text{InMy}_3$  with  $\text{TMSi}_3\text{P}$  in the presence of amines.<sup>1</sup> This intermediate peak is observed to be present when the  $\text{TMGe}_3\text{P}$  precursor is allowed to react without the presence of the  $\text{TMSi}_3\text{P}$  precursor, and a second intermediate is also observed (figure S7). The second intermediate occurs at 0.28ppm and is obscured by the presence of  $\text{TMSi}$ -Myristate in figure 3.

A similar experiment was performed with the two arsenic precursors. However the reaction rate of  $\text{TMSi}_3\text{As}$  was too fast to observe, as no  $\text{TMSi}_3\text{As}$  remained after the NMR tube containing the reaction mixture had been inserted into the NMR spectrometer and the instrument prepared for acquisition (figure S4). However, the reaction of  $\text{TMGe}_3\text{As}$  was readily observed to proceed from  $\text{TMGe}_3\text{As}$  to  $\text{TMGe}$ -myristate. By assuming that the height of any remaining  $\text{TMSi}_3\text{As}$  peak in the NMR spectrum was less than the level of the noise, and because the time between precursor mixing and the acquisition of the first spectrum was  $<1.5$  minutes, we can infer that the rate constant for the reaction of  $\text{TMSi}_3\text{As}$  was at least 30x faster than the reaction rate of  $\text{TMGe}_3\text{As}$  under the same conditions (figure S8). We also found that we could slow the reaction rate by increasing the concentration of TOP, an effect similar to that observed previously with indium phosphide and octylamine (figure S9).<sup>1</sup> In order to further characterize the reaction between  $\text{InMy}_3$  and  $\text{TMGe}_3\text{As}$ , the concentration of  $\text{InMy}_3$  was varied and the reaction order in indium was determined to be second order (figure S10). This result differed from the reaction order determined by observing the absorption rise times with varying concentrations of indium at  $130^\circ\text{C}$  (figure S12). The apparent discrepancy between the reaction order observed using these two sets of conditions and measurement techniques suggests a chemical mechanism that is sensitive to changes in temperature, TOP concentration, or both.

In summary, we have identified two precursors for III-V QD growth that are less reactive and produce particles with improved size distributions. We have shown that  $\text{TMGe}_3\text{As}$  can be used to significantly improve the size distributions of  $\text{InAs}$  QDs and have shown that the

rates of precursor conversion are slower for the  $\text{TMGe}_3\text{V}$  precursors than for their  $\text{TMSi}_3\text{V}$  analogues ( $\text{TMGe}_3\text{P}$  reacted  $\sim 4\times$  more slowly than  $\text{TMSi}_3\text{P}$ , while  $\text{TMGe}_3\text{As}$  reacted at least  $30\times$  more slowly than  $\text{TMSi}_3\text{As}$ ). Although, even with the less reactive precursors, the precursor conversion rates for III-V QDs still occurs on a timescale faster than particle growth, the less reactive arsenic precursor still leads to significant improvements in QD size distribution. This may be because the precursor conversion has been slowed sufficiently that precursor conversion occurs on a timescale slower than mixing. As a result, the size distributions of clusters may be more uniform and therefore result in a more uniform size distribution of QDs following the ripening step. The synthesis of InAs or InP QDs from these new precursors has not yet been optimized, and it is possible that the quality of InP and InAs QDs can be improved further.

## Supplementary Material

Refer to Web version on PubMed Central for supplementary material.

## Acknowledgments

This work was supported in part by the NIH National Cancer Institute Grant (5R01-CA126642), the ARO through the Institute for Soldier Nanotechnologies (W911NF-07-D-0004), DARPA (P010053329), and the NSF through a Collaborative Research in Chemistry Program (CHE-0714189). The work also made use of the DCIF at MIT which is supported by the NSF (CHE-9808061). D.K.H. was supported by a NSF Graduate Research Fellowship. Special thanks to Brian Walker, Peter Allen, Jose Cordero, and Hee Sun Han for helpful discussions and to Jeffrey Simpson for assistance with NMR data processing and kinetics measurements.

## References

1. Allen PM, Walker BJ, Bawendi MG. *Angew Chem, Int Ed.* 2010; 49:760–2.
2. Liu H, Owen JS, Alivisatos AP. *J Am Chem Soc.* 2007; 129:305–12. [PubMed: 17212409]
3. Steckel JS, Yen BKH, Oertel DC, Bawendi MG. *J Am Chem Soc.* 2006; 128:13032–3. [PubMed: 17017765]
4. Owen JS, Chan EM, Liu H, Alivisatos AP. *J Am Chem Soc.* 2010; 132:18206–13. [PubMed: 21128655]
5. Clark MD, Kumar SK, Owen JS, Chan EM. *Nano Lett.* 2011; 11:1976–80. [PubMed: 21476514]
6. Cossairt BM, Owen JS. *Chem Mater.* 2011; 23:3114–3119.
7. Joung S, Yoon S, Han CS, Kim Y, Jeong S. *Nanoscale Res Lett.* 2012; 7:93. [PubMed: 22289352]
8. Amberger E, Salazar R. *J Organomet Chem.* 1967; 8:111–114.
9. Atesa M, Breuniga H, Denkera M. *Phosphorus, Sulfur Silicon Relat Elem.* 1995; 102:287–289.
10. Allen PM, Liu W, Chauhan VP, Lee J, Ting AY, Fukumura D, Jain RK, Bawendi MG. *J Am Chem Soc.* 2010; 132:470–1. [PubMed: 20025222]
11. Leatherdale CA, Mikulec FV, Bawendi MG. *J Phys Chem B.* 2002; 106:7619–7622.

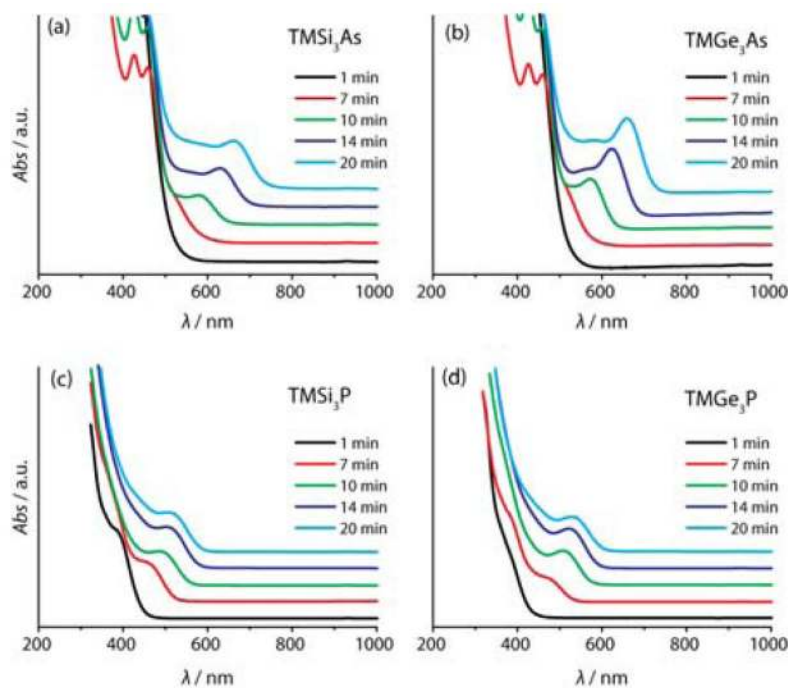


**Figure 1.** Absorption spectra of aliquots taken during growth of InAs (a, b) and InP (c, d) using the silyl-V precursor (a, c) and the germyl-V precursor (b, d)

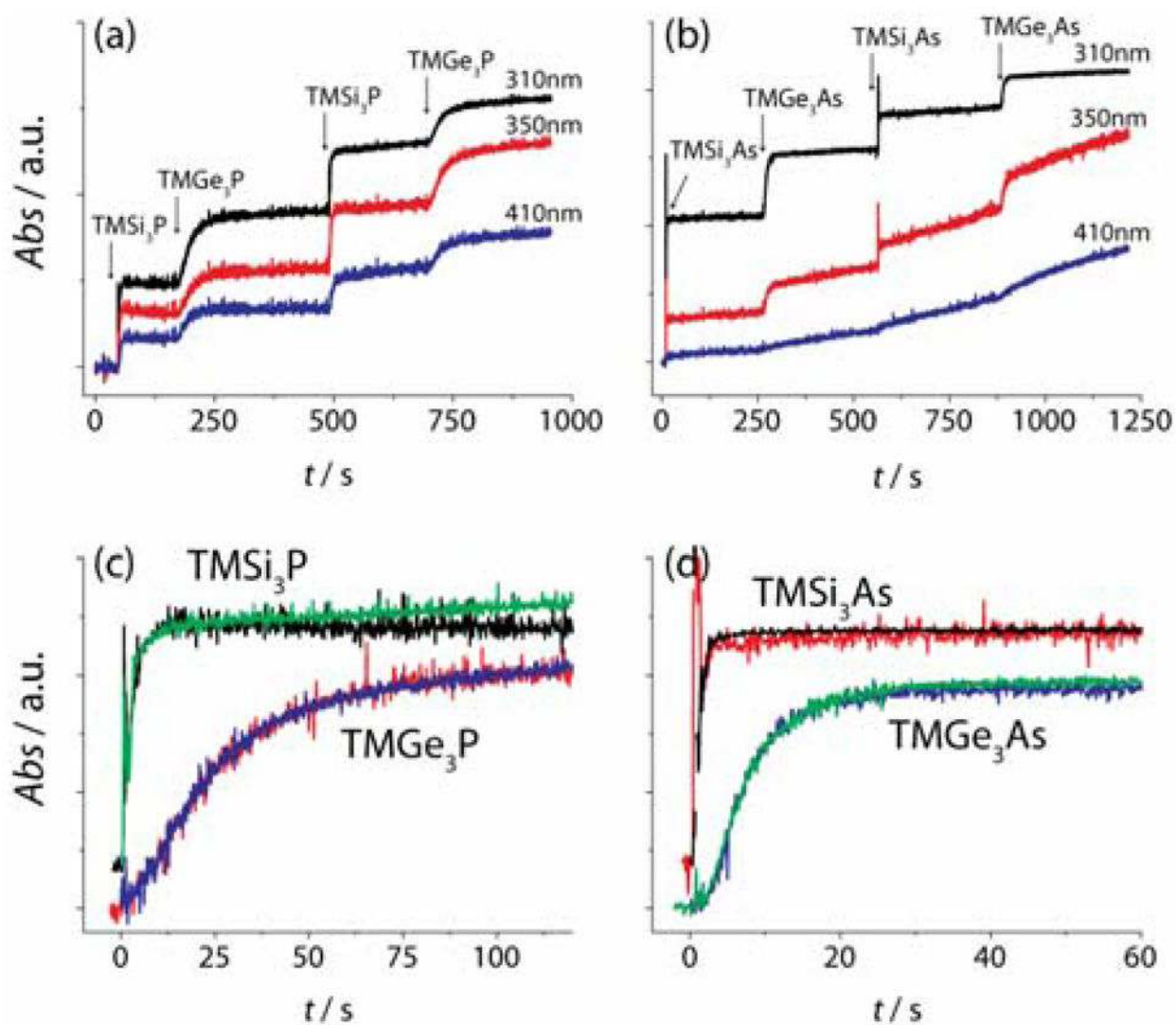


**Figure 2.** Absorbance traces during precursor injection at 130°C for InP (a) and InAs (b). The injection of silyl-V and germyl-V precursor was alternated so that the absorbance rise could be directly compared. The absorbance rise at 310 nm (from a, b) is normalized truncated, and adjusted so that each injection is plotted with  $t=0$  (c, d). The TMSi<sub>3</sub>V precursor injections in c and d are offset for clarity.

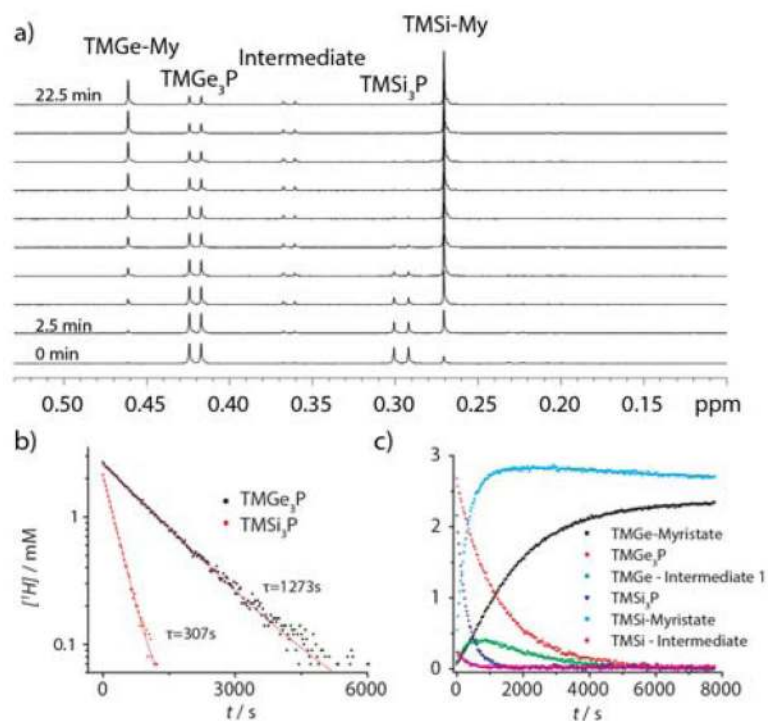


**Figure 3.**

A time series of NMR spectra showing simultaneous reaction of TMSi<sub>3</sub>P and TMGe<sub>3</sub>P with 2.5mM InMy<sub>3</sub> (a), integrated peak area for TMSi<sub>3</sub>P and TMGe<sub>3</sub>P normalized and plotted on a semilog plot (b), and integrated peak areas normalized by total proton concentration associated with the corresponding TME-peaks (c).